The effect of reinforcement position on geogrid reinforced clay liners

D.H. Marx. Jones & Wagener Engineering & Environmental Consultants (formerly University of Pretoria), South Africa. marxdavidh@gmail.com
S.W. Jacobsz. Department of Civil Engineering, University of Pretoria, South Africa.
sw.jacobsz@up.ac.za

ABSTRACT
Differential settlement and local voids below landfill liners can result in the liners distorting and cracking. By using geogrids as reinforcement the effect of the voids, or differential settlement can be mitigated. The geogrid both increases the stiffness of the system - reducing its distortion - and decreases the tensile stress at the crack tips –stunting crack growth. Reinforced clay liners subject to differential settlement were modelled in a geotechnical centrifuge. Top-, bottom- and unreinforced liners were modelled to investigate the effect of reinforcement position on the response of the liners while settling. It was found that the severity of the cracks and tensile and compressive strain concentrations were reduced when the reinforcement was placed in the top of the liner, compared to bottom reinforced and unreinforced liners.

1. INTRODUCTION

Clay barriers are commonly used to isolate areas used for the disposal of hazardous waste from the surrounding environment. Local voids forming in the waste below the liner, or differential settlement of the waste, can distort the liner and result in fracture. Once the clay liner cracks its permeability increases and its ability to perform as a barrier is compromised. Two of the most vulnerable types of liners are capping liners and liners in piggyback landfills. In piggyback landfills a new, lined landfill is constructed on top of an existing waste dump. The old waste dump is usually a soft, heterogeneous mass prone to differential settlement.

Geogrid reinforcement can be used to mitigate the effect of differential settlement, or void formation, on the liners. The geogrid enhances the clay liner by increasing the stiffness of the system, thus decreasing the settlement and distortion. Furthermore, with sufficient bond between the geogrid and the clay, the geogrid will be in tension, moving the neutral axis of the composite beam upwards and reducing the tensile stress in the clay.

A number of different positions for placing reinforcement in deflecting clay liners have been suggested. Giroud (1981) used basal reinforcement for his calculation of a geogrid spanning a void. Viswanadham (1996) found reinforcement in the top quarter of a capping layer to be more effective than at the base. In literature outside of clay liners Kuo & Hsu (2003) found that placing reinforcement 1/3rd from the top of a pavement was effective. Finally, from triaxial tests on railway ballast Mishra et al. (2014) recommend placing reinforcement 2/5^{ths} from the top, and 2/5ths from the bottom of a soil layer.

Full scale tests investigating reinforced clay liners are expensive and time consuming. Consequently, centrifuge tests has often been used to study clay liners subject to settlement (Jessberger & Stone, 1991; Viswanadham & Jessberger, 2005; Viswanadham & Muthukumaran, 2007; and Rajesh & Viswanadham, 2009, 2011, 2012). The centrifuge tests were used to identify the key mechanisms governing the behaviour of a reinforced liner subjected to differential settlement. Both liners with and without overburden pressure was tested. To observe these mechanisms the strain along the side of the liner can be measured.

For this study three centrifuge tests of clay liners subject to differential settlement were conducted. The tests were of an unreinforced liner, a liner reinforced at the top quarter and a liner reinforced at the bottom quarter. The effect of the different reinforcement positions was evaluated in terms of the strain distributions in the liners.

2. METHODOLOGY

Centrifuge modelling entails constructing a 1/N scale model of a prototype (full scale) problem. By increasing the gravitational acceleration of the model N times the stress in the model will be equivalent to the prototype model. As the stress in the model is the same as the prototype it can be assumed that its behaviour mirrors that of the prototype. Consequently, the technique of centrifuge modelling allows for the study of problems that would be impractical to model in full scale.

2.1 Model setup and test procedure

The geotechnical centrifuge of the University of Pretoria (Jacobsz et al., 2014) was used to model reinforced clay liners subject to differential settlement. A 600 mm long centrifuge strongbox with a glass window in the front was used for the tests. A divider was placed 150 mm behind the window to confine the clay.

The model consisted of a 30 mm thick clay liner, underlain by a 100 mm layer of sacrificial sand layer, on top of a trapdoor supported by a central piston (see Figure 1). As the piston lowered a void formed below the clay liner, inducing distortion. The sacrificial sand layer reduced the strain concentrations on the liner by smoothing out the deflected profile. At 30g (the acceleration used for these test) the setup modelled a 7.98 m wide void with 5.01 m support to either side with a maximum settlement of 1.5 m. The 30 mm thick model liners was equivalent to a 900 mm thick liner at 30g. As overburden pressure suppresses crack formation (Jessberger & Stone, 1991, Viswanadham & Majesh, 2002), it was not modelled to allow for better observation of the fracture behaviour of the liners.

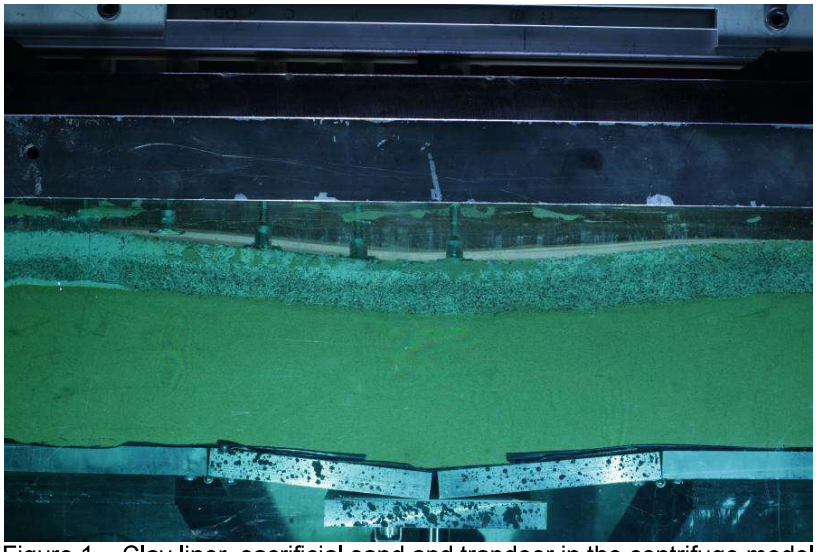

Figure 1 – Clay liner, sacrificial sand and trapdoor in the centrifuge model

At the start of each test the models were gradually accelerated to 30g. Once the acceleration reached 30g, the clay was allowed to consolidate and the hydraulic system was equilibrated for 15 min. Subsequently, the central platform was lowered at a rate of 1 mm/min for 5 min, and thereafter at 3 mm/min for the remainder of the test. The initial settlement rate of 1 mm/min was to allow for the studying of the arching behaviour of the sand at small movements. Thereafter the settlement rate was increased to ensure that behaviour of the clay remained undrained. During the test a Canon 100D SLR camera fitted with a 40 mm fixed lens was used to capture photos of the liners.

2.2 Materials used

The sand of the sacrificial layer had a friction angle of 50° and c' of 0 kPa at a relative density of 50%. The specific gravity of the sand was 2.666. A grading curve of the sand is shown in Figure 2. Detailed properties of the sand can be found in Archer (2014).

The clay liner was constructed as a homogeneous layer of consolidated kaolin clay. Pure kaolin was used to ensure a repeatable preparation procedure. Furthermore, Jessberger & Stone (1991) found little difference in the behaviour of a model liner prepared by consolidated the clay liner and one prepared by compacting the clay.

The kaolin clay used for this study was obtained from the Gujurat province of India. It had a liquid limit of 37%, a plasticity index of 9% and a specific gravity of 2.662. The particle size distribution of the clay is shown in Figure 2. To construct the model liners the clay was one-dimensionally consolidated to 610 kPa. This consolidation stress is equivalent to a 95% Proctor density of 1416 kg/m³. After the model liner was trimmed to 30 mm thick, the side facing the glass window of the centrifuge strongbox was covered with sand to improve subsequent DIC analyses.

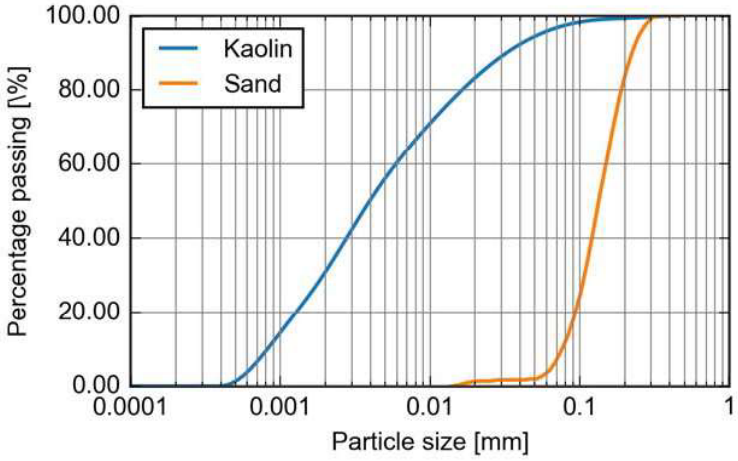

Figure 2 – Grading of the sand and kaolin clay.

The reinforced liners were constructed by first consolidating the bottom half of the liner, then placing the model geogrid and finally consolidating another layer of clay on top. For the bottom reinforced test the reinforcement was placed a quarter from the bottom of the liner, and for the top reinforced liner one quarter from the top.

The Huesker HaTe 23.142 mesh shown in Figure 3 was used as a model geogrid for the reinforced liners. Viswanadham & König (2004) developed a number of scaling laws to determine the equivalent prototype behaviour of a model geogrid at increased acceleration in a centrifuge. At 30g a prototype geogrid with 10 mm wide ribs should be modelled by mesh with ribs of 0.333 mm wide. Consequently, due to practical considerations the model geogrids used in centrifuge models typically represents geogrids stronger than those used in design at increased acceleration. The polyethylene terephthalate (PET) HaTe mesh used in this study has an equivalent prototype stiffness of 2876 kN/m at 1% strain and 2734 kN/m at 3% strain. At 30g the model geogrid represented a prototype with 10.5 mm thick ribs that are 18.3 – 27.3 mm wide and had apertures of 90 mm x 90 mm. As clay cracks at much lower strain than the failure strain of geogrids, the ultimate strength of the model geogrid was not relevant. Furthermore, centrifuge tests does rarely last longer than a couple of hours and thus the durability of the model geogrids was not of concern.

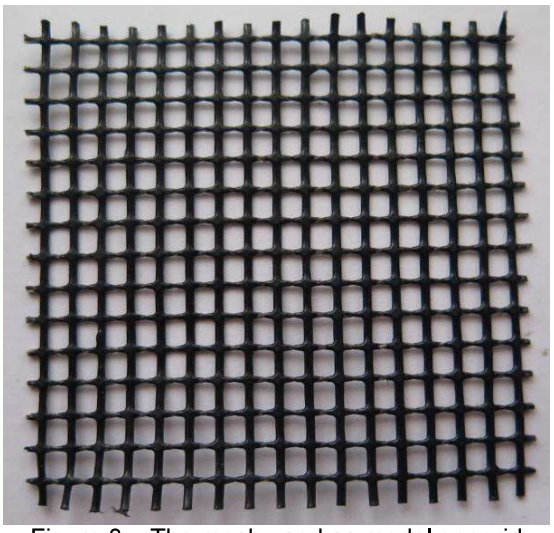

Figure 3 – The mesh used as model geogrid

2.3 Strain measurements with Digital Image velocimetry

To calculate the strain in the liners during the centrifuge tests Digital Image Correlation (DIC) was implemented. DIC entails the analysis of digital images of the liner captured as it settles in the centrifuge. The position of a soil particle is tracked from one image to another to determine its displacement. This process is repeated for a number of patches of soil particles across the liner to generate a displacement field. Finally the displacement fields are used to calculate strain fields across the model liners. The GeoPIV-RG software by Stanier et al. (2015) was used for this study.

3. RESULTS

Firstly, surface laser scans of the centrifuge tests are presented as an indication of the severity of the cracks that formed. Thereafter the tensile and compressive horizontal strains in the different model liners are discussed.

3.1 Surface laser scans

The surface of each of the liners was surveyed at the end of each test with a Micro-Epsilon scanCONTROL 2900-100 laser scanner. In Figure 4a a photo of the side of the unreinforced liner at the end of the test is shown. In Figure 4b the corresponding surface scan for the unreinforced liner is presented. Figure 4c and d shows surface scans for the bottom reinforced and top reinforced liners at the end of the respective tests. For all liners at least one crack extended from the front of the liner through to the back at the end of each test (1.5 m central settlement). However, the cracks for the unreinforced and bottom reinforced liners (Figure 4b & c) were significantly more severe than the top reinforced liner (Figure 4d). Furthermore, the top-reinforced liner had only one significant crack – on the right – with only minor cracks forming on the left. The laser scans and photos of the liners were used to identify the locations where cracks formed in each of the liners. At these locations the strain fields in the different liners were compared.

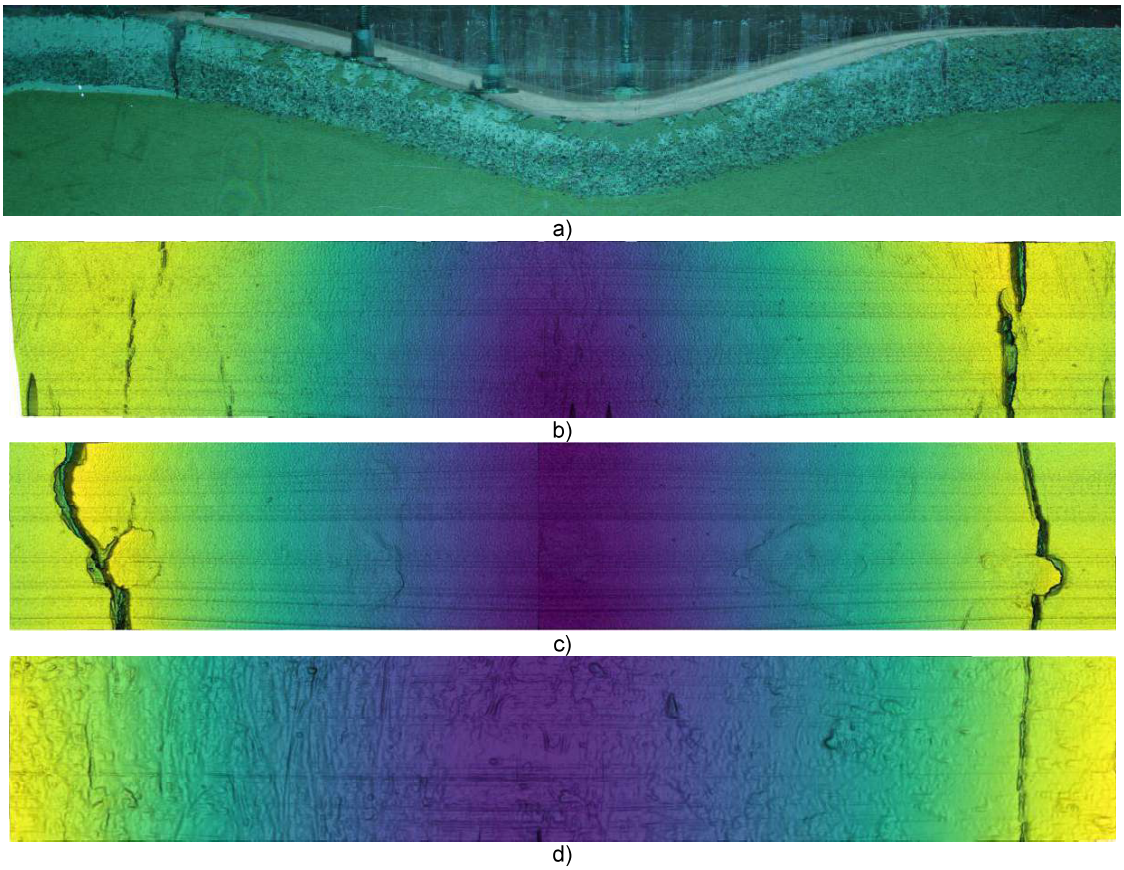

Figure 4 - Photo (a) and laser surface scan (b) of the unreinforced liner at the end of the test. Laser surface scans of the (c) the bottom reinforced and (d) the top reinforced liner at the end of the test.

3.2 Strain distributions

Micro cracks formed in the unreinforced, bottom-reinforced and top-reinforced liners at different central settlements. The origin of the micro-cracks was identified from a change in horizontal strain along the top edge of the liners. The micro-cracks formed at settlements of 4.06, 7.88 and 12.7 mm for the different liners. At each of the three displacements strain fields across the side of the liner were calculated with the GeoPIV-RG software. However, during the initial acceleration of the centrifuge all the liners displaced slightly due settlement of the sacrificial sand and slack in the hydraulic system. As no photos were available during this process the displacement fields from the DIC analyses did not include the initial displacement of the liners. Consequently, the strain calculated for the liners was not the absolute strain of the liners but rather relative to the strain due to the initial displacement.

To ensure that the relative strain results of the different liners was comparable it was firstly scaled by the minimum and maximum values in each of the liners at a central settlement of 12.7 mm. However, due to the presence of wild vectors (incorrect displacement vectors calculated by the DIC software) outliers were present in the strain fields. Consequently, these outliers were first removed from the data using the skewed box-and-whiskers plot of Hubert & Vandervieren (2008) from the field of *Robust Statistics* Rousseeuw & Hubert, 2011). Subsequently, the minimum and maximum strains were identified and the strain fields scaled by $\varepsilon^* = (\varepsilon - \varepsilon_{min})/(\varepsilon_{max} - \varepsilon_{min})$.

Scaled linear horizontal strain across the side of each of the liners is shown in Figure 5 for a central settlement of 12.7 mm. The zones of major tensile strains (left and right hogging), as well as the zone of maximum compressive strain (centre sagging) are indicated for each liner.

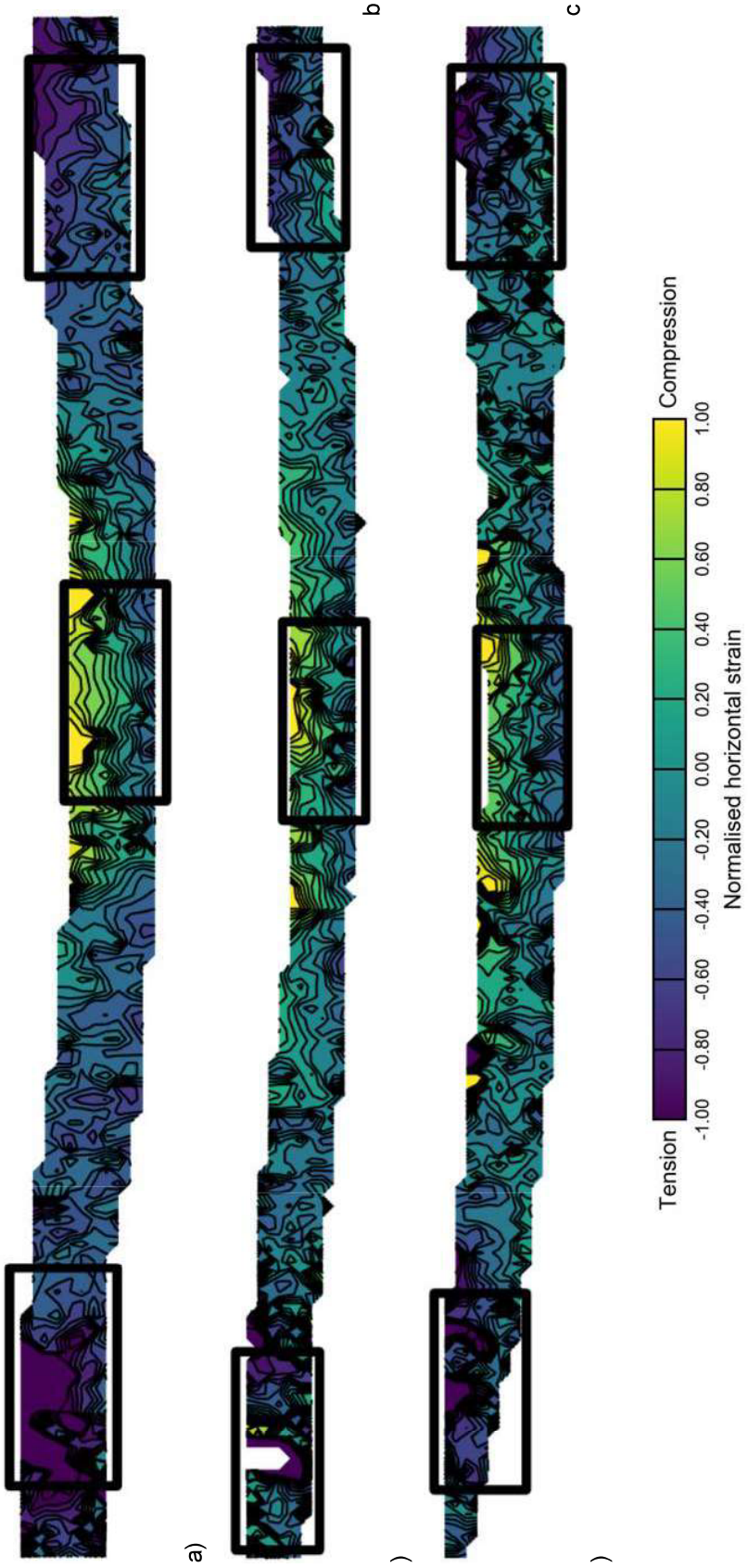

Figure 5 - Linear horizontal strain for a central settlement of 12.7 mm for a) a unreinforced, b) a bottom reinforced and c) top-reinforced liner.

Consider the horizontal strain in the left hogging zone of the three liners for central settlements of 4.06, 7.88 and 12.7 mm, as shown in Figure 6. At a central settlement of 4.06 mm micro cracks were identified in the unreinforced liner. Similarly, significant tensile strain concentrations are visible in the left hogging zone of the unreinforced liner. At the second comparison point of 7.88 mm significant tensile strain concentrations are present in both the unreinforced and top reinforced liners. These concentrations extends from the surface of the liners to the base, indicating that catastrophic failure is imminent. Similarly, the photos of the liner at the end of the tests shows severe cracks extending from the surface of the liners downwards. For the bottom reinforced liner these cracks terminated at the position of the reinforcement.

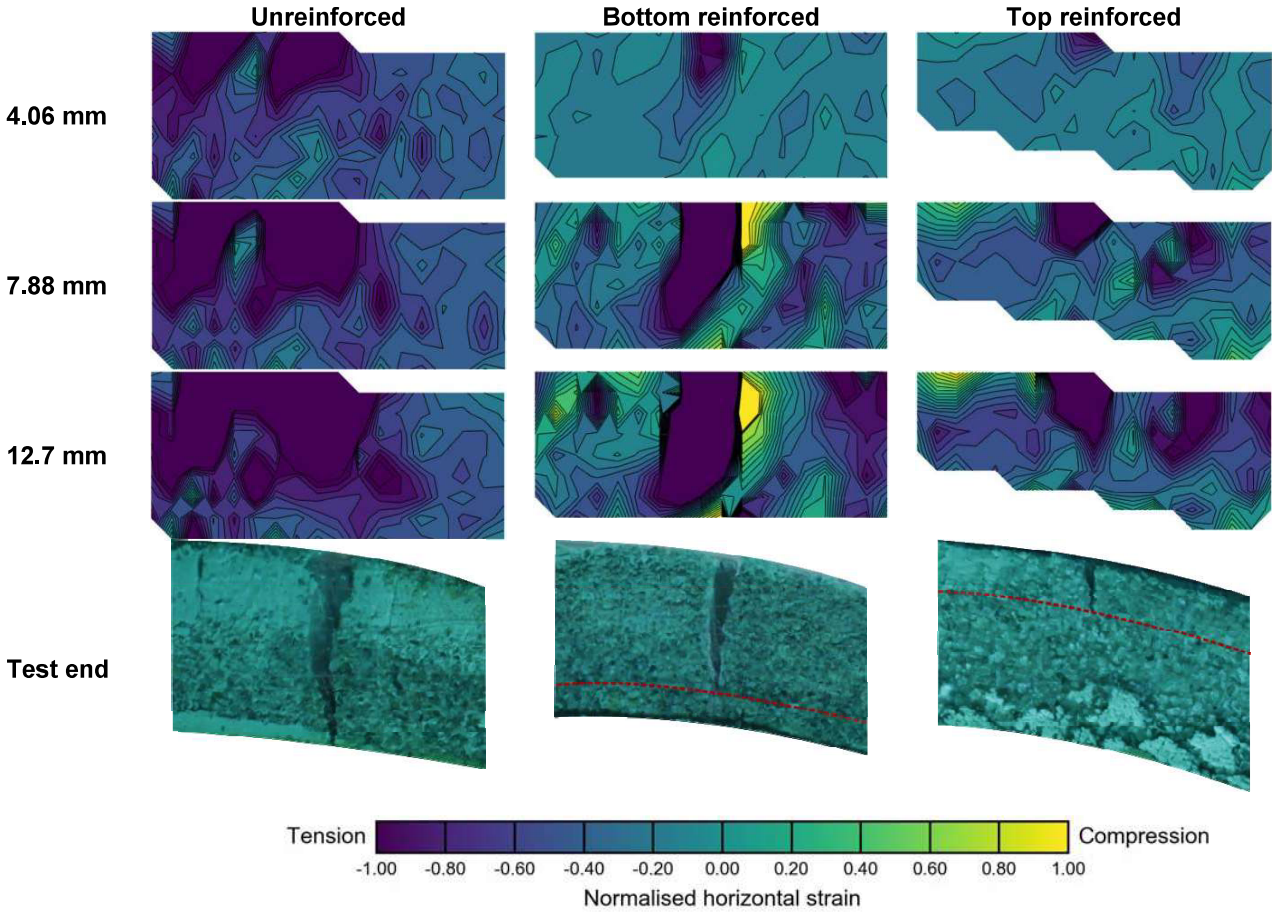

Figure 6 - Fracture and tensile strain concentrations in the liners for hogging at different settlements.

Geogrids in reinforced liners has some initial slack as they installed without any tension. Consequently, only once the geogrid strains does it mobilise strength and increase the stiffness of the system. For the bottom reinforced liner a significant crack propagated through the liner before the strength of the geogrid was mobilised. Consequently, the strain concentrations in the bottom reinforced liner was similar to that of the unreinforced liner. Only once the crack reached the geogrid did it reduce the tensile stress at the crack tip, and was crack growth terminated.

In contrast, for the top reinforced liner significant strain concentrations extended only through the top quarter of the liner, before it stopped at the level of the geogrid. These strain concentrations are visible only at a central displacement of 12.7 mm (compared to 4.06 and 7.88 mm for the other liners) indicating that the geogrid increased the stiffness of the system. Consequently, the liner's deflection for a given central settlement was reduced, and thus the strain in the model liners as well.

Likewise, the compressive strain in the top-reinforced liner is lower than in both the unreinforced and bottom-reinforced liners. In Figure 7 the strain at the sagging region of each of the liners is shown for central displacements of 4.06, 7.88 and 12.7 mm. At a central settlement of 7.88 mm the compressive strain in the unreinforced and top-reinforced liners is greater than the tensile strain. However, for the top-reinforced liner the compressive strain remained in balance with the tensile. Finally, when the unreinforced liner cracked through the compressive stress was great enough to result in a compressive failure of the liner. This compressive failure is visible in the surface laser scan in Figure 8.

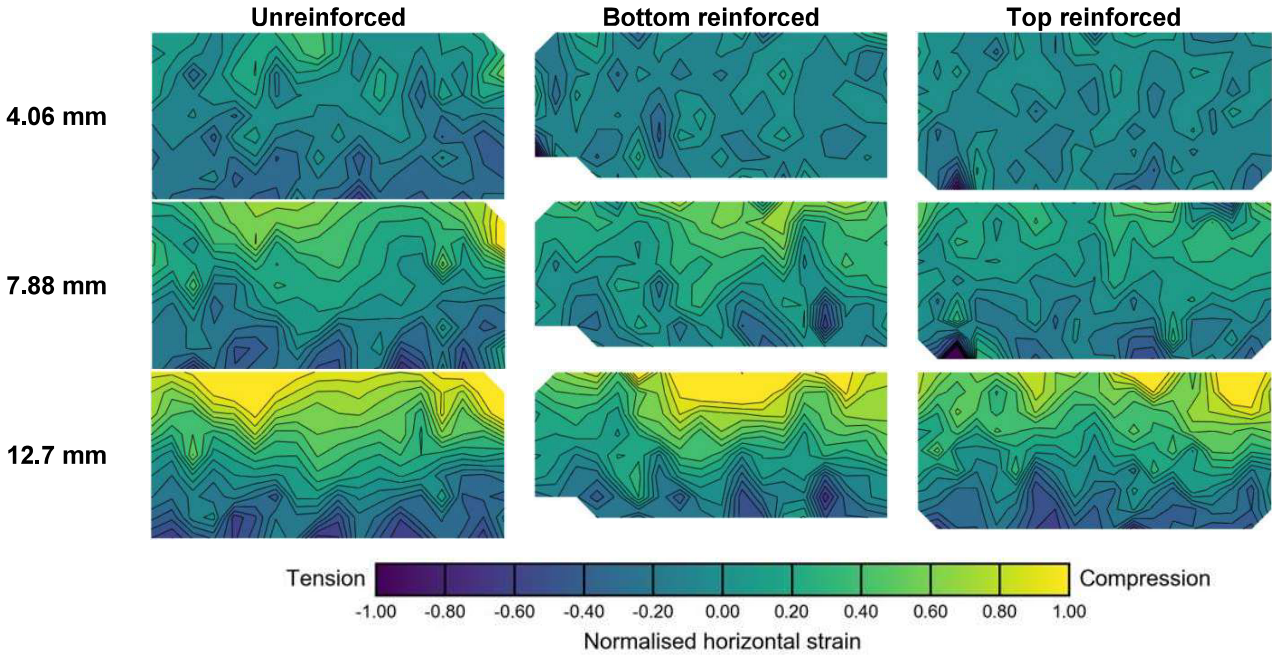

Figure 7 – Compressive strain concentrations for sagging at different settlements in the three liners.

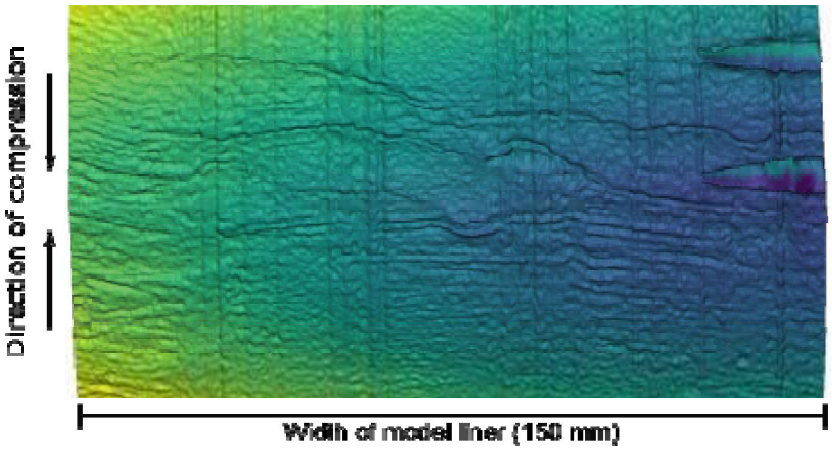

Figure 8 - Compressive failure in the centre of the unreinforced liner.

4. CONCLUSIONS

Centrifuge tests of clay liners were done to determine the effect of reinforcement position on the behaviour of reinforced liners subjected to differential settlement. In surface laser scans of the model liners similar cracks were observed in the unreinforced and bottom reinforced liners. Furthermore, both these liners had tensile strain concentrations extending from the surface to the base of the liner. The strain fields are indicative of potential cracks.

In contrast to the unreinforced and bottom reinforced liners, significantly smaller cracks were observed on the surface of the top-reinforced liner. Furthermore, the tensile strain concentrations extended only through the top quarter of the liner and the compressive strain concentrations were significantly less severe. Consequently, it is recommended that top reinforcement rather than bottom reinforcement should be implemented for design cases where differential settlement, rather than severe voids directly below the liner is expected. It is, however, recommended that double reinforcement of the liners should also be investigated as top reinforcement of the liners will only be effective when the liner does not span the void.

ACKNOWLEDGEMENTS

The financial assistance of the Deutscher Akademischer Austausch Dienst (DAAD), the National Research Foundation of South Africa (NRF) and the Geosynthetics Interest Group of South Africa (GIGSA) is acknowledged by the first author. Opinions expressed and conclusions presented are those of the authors and are not necessarily to be attributed the NRF or GIGSA.

REFERENCES

Archer, A. (2014). Using small-strain stiffness to predict the settlement of shallow foundations on sand. MEng dissertation. University of Pretoria.

Kuo, C. & Hsu, T. (2003). Traffic induced reflective cracking on pavements with geogrid-reinforced asphalt concrete overlay. *Proceedings of the 82th Annual Meeting at the Transportation Research Board*.

Mishra, D., Qian, Y., Kazmee, H. & Tutumluer, E. (2014). Investigation of Geogrid-Reinforced Railroad Ballast Behavior Using Large-Scale Triaxial Testing and Discrete Element Modeling. *Transportation Research Record: Journal of the Transportation Research Board*, No. 2462, pp 98–108.

Giroud, J.-P. (1981). Designing with geotextiles. *Matériaux et Constructions*, Vol. 14, No. 82, pp. 257–272.

Hubert, M. & Vandervieren, E. (2008). An adjusted boxplot for skewed distributions. *Computational Statistics and Data Analysis*, Vol. 52, No. 12, pp. 5186–5201.

Jacobsz, S., Kearsley, E. & Kock, J. (2014). The geotechnical centrifuge facility at the University of Pretoria. *Proceedings of the 8th International Conference on Physical Modelling in Geotechnics 2014*. Perth, Australia: CRC Press.

Jessberger, H. & Stone, K. (1991). Subsidence effects on clay barriers. *Géotechnique*, Vol. 41, No. 2, pp. 185–194.

Rajesh, S. & Viswanadham, B. (2009). Evaluation of geogrid as a reinforcement layer in clay based engineered barriers. *Applied Clay Science*, Vol. 46, No. 2, pp. 153–165.

Rajesh, S. & Viswanadham, B. (2011). Hydro-mechanical behavior of geogrid reinforced soil barriers of landfill cover systems. *Geotextiles and Geomembranes*, Vol. 29, No. 1, pp. 51–64.

Rajesh, S. & Viswanadham, B. (2012). Centrifuge Modeling and Instrumentation of Geogrid-Reinforced Soil Barriers of Landfill Covers. *Journal of Geotechnical and Geoenvironmental Engineering*, Vol. 138, No. 1, pp. 26–37.

Rousseeuw, P. & Hubert, M. (2011). Robust statistics for outlier detection. *Wiley Interdisciplinary Reviews: Data Mining and Knowledge Discovery*, Vol. 1, No. 1, pp. 73–79.

Stanier, S., Blaber, J, Take,W. A. & White, D. (2015). Improved image-based deformation measurement for geotechnical applications. Canadian Geotechnical Journal, Vol. 13, pp. 1–35.

Viswanadham, B. (1996). *Geosynthetic reinforced mineral sealing layers of landfills*. Phd. Bochum, Germany: Ruhr University.

Viswanadham, B. & König, D. (2004). Studies on scaling and instrumentation of a geogrid. *Geotextiles and Geomembranes*, Vol. 22, No. 5, pp. 307–328.

Viswanadham, B. & Jessberger, H. (2005). Centrifuge Modeling of Geosynthetic Reinforced Clay Liners of Landfills. *Journal of Geotechnical and Geoenvironmental Engineering*, Vol. 131, No. 5, pp. 564–574.

Viswanadham, B. & Mahesh, K. 2002. Modeling deformation behaviour of clay liners in a small centrifuge. *Canadian Geotechnical Journal* ,Vol. 39, No. 6, pp. 1406–1418

Viswanadham, B. & Muthukumaran, A. (2007). Influence of geogrid layer on the integrity of compacted clay liners of landfills. *Soils and Foundations*, Vol. 47, No. 3, pp. 517–532.